Universiteit
Leiden
The Netherlands

Biomimetic models of [NiFe] hydrogenase for electrocatalytic hydrogen evolution

Gezer, G.

Citation
Gezer, G. (2017, October 10). *Biomimetic models of [NiFe] hydrogenase for electrocatalytic hydrogen evolution*. Retrieved from https://hdl.handle.net/1887/58770

Version:	Not Applicable (or Unknown)
License:	Licence agreement concerning inclusion of doctoral thesis in the Institutional Repository of the University of Leiden
Downloaded from:	https://hdl.handle.net/1887/58770

Note: To cite this publication please use the final published version (if applicable).

Cover Page

Universiteit Leiden

The handle http://hdl.handle.net/1887/58770 holds various files of this Leiden University dissertation

Author: Gezer, G.
Title: Biomimetic models of [NiFe] hydrogenase for electrocatalytic hydrogen evolution
Issue Date: 2017-10-10

Appendix I

Details of GC and CV Measurements for H_2 Evolution

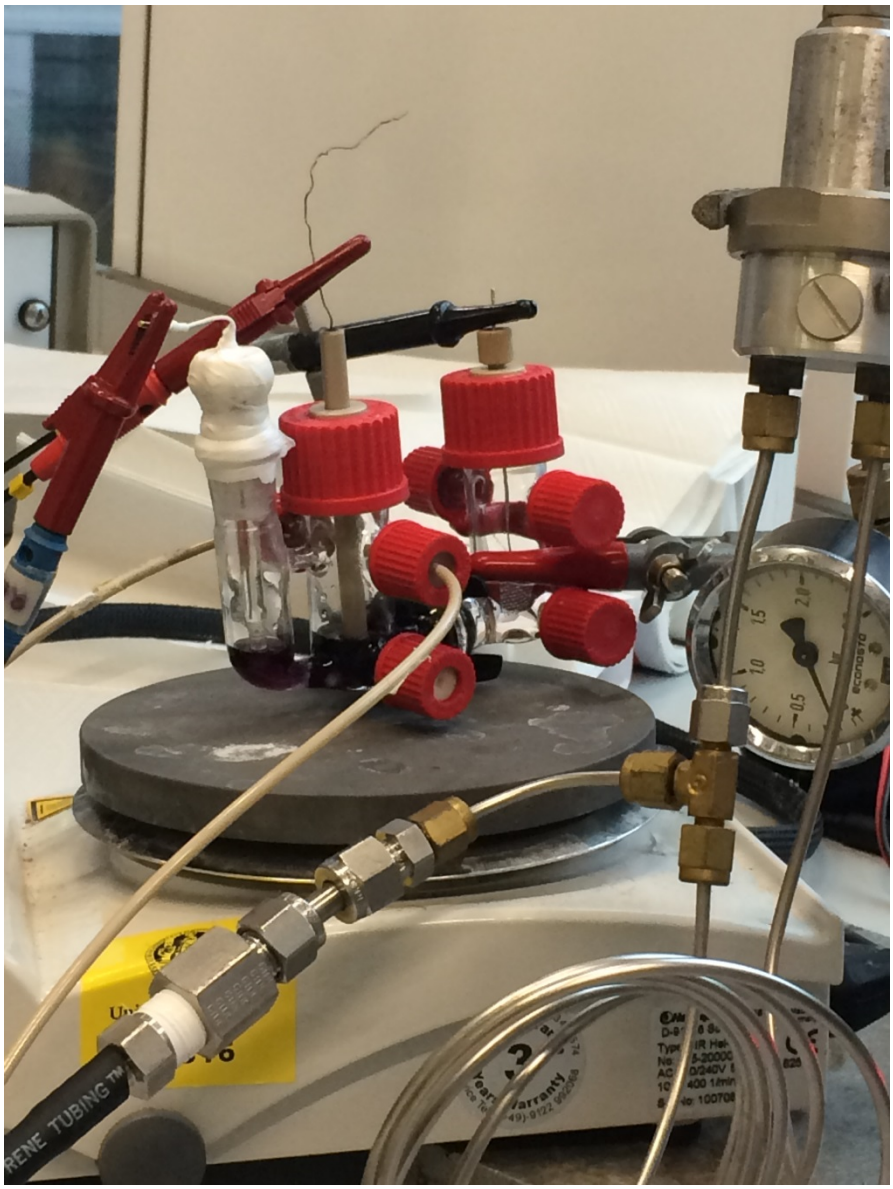

Figure AI.1: Photograph of the controlled-potential coulometry (CPC) experiment setup.

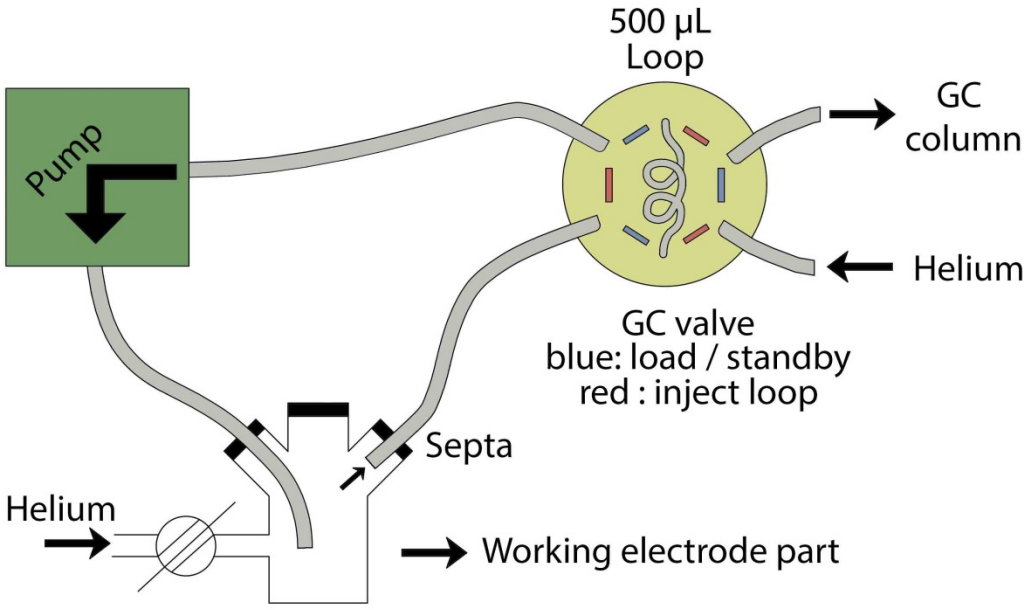

Figure AI.2: Schematic drawing of hydrogen evolution setup.

Hydrogen evolution experiments were done with the three-electrode cell system and electrodes (Figure AI.1). Schematic drawing of the connection from working electrode compartment to the GC setup is shown in Figure AI.2. The reactor is magnetically stirred during the electrolysis. Prior to each measurement the system was deaerated by bubbling with helium for 10 min, while having the pump running. The GC valve and the pump (KNF NMS 010 L micro diaphragm pump) were enclosed in a helium-purged housing to prevent air from leaking into the system. Samples are taken by switching the GC valve from load position (blue) to the inject position (red) while pump is switched off.

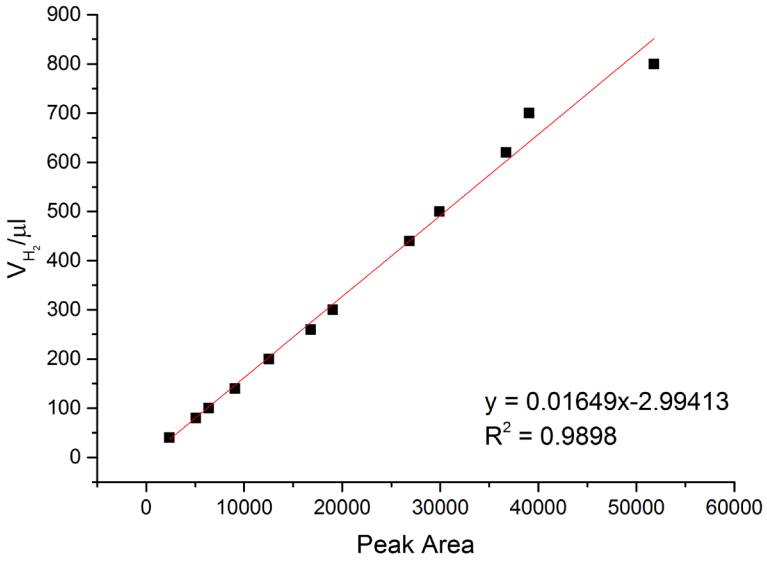

Figure AI.3: Calibration line used for CPC experiments. The observed peak areas of the GC are plotted against the volume of H_2 in the sample with an R^2 value of 0.9898.

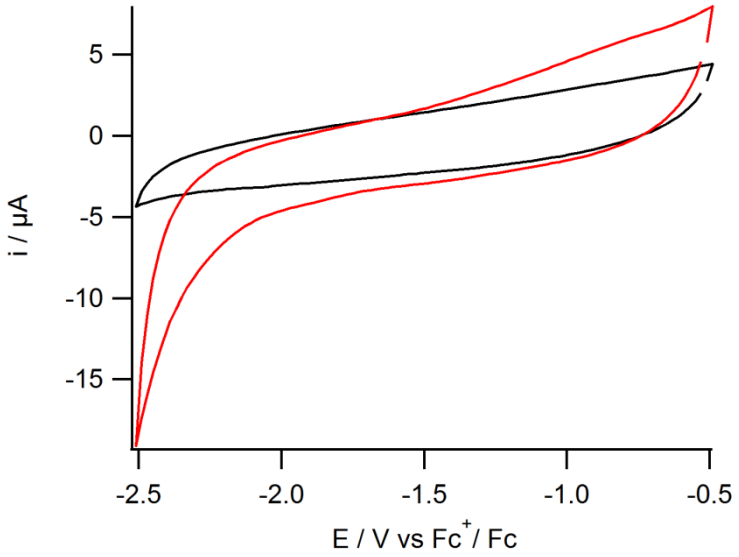

Figure AI.4: Cyclic voltammogram of $TBAPF_6$ (0.1 M) in DMF solution with a glassy carbon working electrode at 200 mV s^{-1} in the presence of 0 (black), 60 (red) mM of acetic acid.

Appendix II

Supplementary Information on Chapter 2

Table AII.1: Crystal and structure refinement data for complexes **(3)**, **(5)** and **(6)**

Data were collected at 110 K using a SuperNova, Dual, Cu at zero, Atlas. H-atom parameters were constrained.

	(3)	**(5)**	**(6)**
Crystal data			
Chemical formula	$C_{11}H_{22}NiS_2Se_2$	$C_{17}H_{27}FeNiOS_2Se_2 \cdot F_6P$	$C_{22}H_{29}FeNiOS_2Se_2 \cdot F_6P \cdot CH_2Cl_2$
M_r	435.03	728.95	875.95
Crystal system, space group	Monoclinic, $P2_1$	Trigonal, R-3:H	Monoclinic, $P2_1/c$
a, b, c (Å)	7.2301 (2), 10.3586 (2), 10.5707 (3)	31.5009 (7), 31.5009 (7), 14.4145 (4)	10.32665 (13), 22.8030 (2), 13.72057 (17)
α, β, γ (°)	90, 103.465 (3), 90	90, 90, 120	90, 105.9916 (13), 90
V (Å^3)	769.92 (4)	12387.3 (6)	3105.87 (6)
Z	2	18	4
Radiation type	Mo $K\alpha$	Cu $K\alpha$	Cu $K\alpha$
μ (mm^{-1})	6.23	10.52	11.00
Crystal size (mm)	0.26 × 0.19 × 0.03	0.18 × 0.05 × 0.04	0.36 × 0.08 × 0.04

	(3)	(5)	(6)
Data collection			
T_{min}, T_{max}	0.316, 0.839	0.414, 0.788	0.161, 0.716
No. of measured, independent and observed [$I > 2\sigma(I)$] reflections	11826, 3544, 3416	16503, 5401, 4525	20451, 6094, 5655
R_{int}	0.030	0.032	0.033
$(\sin \theta/\lambda)_{max}$ (Å^{-1})	0.649	0.616	0.616
Refinement			
$R[F^2 > 2\sigma(F^2)]$, $wR(F^2)$, S	0.022, 0.050, 1.04	0.039, 0.084, 1.06	0.030, 0.077, 1.03
No. of reflections	3544	5401	6094
No. of parameters	149	284	405
No. of restraints	1	0	181
	$w = 1/[\sigma^2(F_o^2) + (0.0249P)^2 + 0.0526P]$ where $P = (F_o^2 + 2F_c^2)/3$	$w = 1/[\sigma^2(F_o^2) + (0.0255P)^2 + 67.0697P]$ where $P = (F_o^2 + 2F_c^2)/3$	$w = 1/[\sigma^2(F_o^2) + (0.0416P)^2 + 2.5519P]$ where $P = (F_o^2 + 2F_c^2)/3$
$\Delta\rho_{max}$, $\Delta\rho_{min}$ (e Å^{-3})	0.47, -0.33	0.47, -0.92	0.90, -0.89

Computer programs: *CrysAlis PRO*, Agilent Technologies, Version 1.171.36.32 (release 02-08-2013 CrysAlis171 .NET) (compiled Aug 2 2013, 16:46:58), *SHELXS2014*/7 (Sheldrick, 2015), *SHELXS2014*/7 (Sheldrick, 2014), *SHELXL2014*/7 (Sheldrick, 2015), *SHELXL2014*/7 (Sheldrick, 2014), *SHELXTL* v6.10 (Sheldrick, 2008).[1]

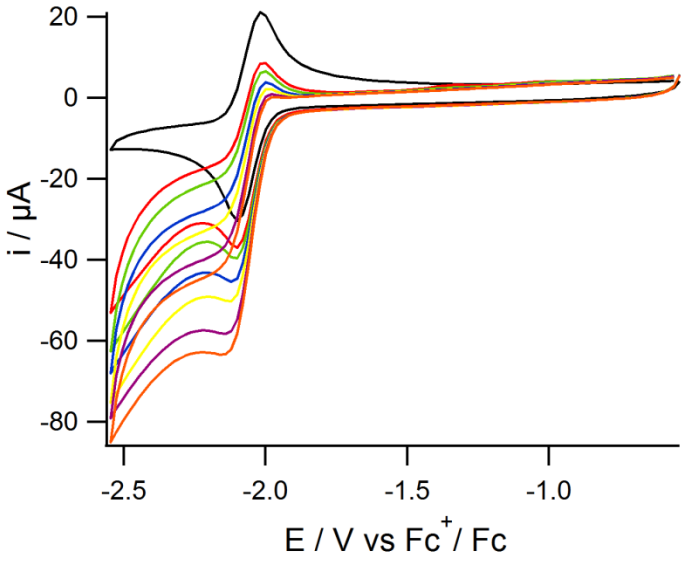

Figure AII.1: Cyclic voltammogram of [Ni(pbSmSe)] **(3)** (1mM) in a DMF solution of $TBAPF_6$ (0.1 M) using a glassy carbon electrode at 200 mV s^{-1} with 0 (black), 10 (red), 20 (green), 30 (blue), 40 (yellow), 50 (purple), 60 (orange) mM of acetic acid.

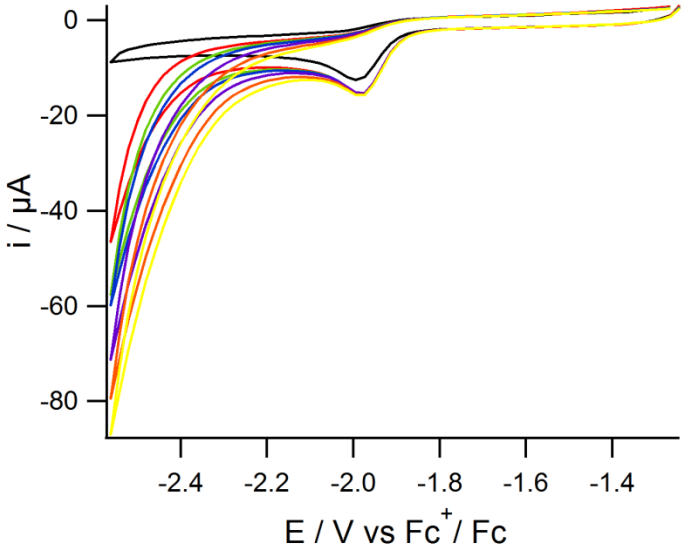

Figure AII.2: Cyclic voltammogram of [Ni(xbSmSe)] **(4)** (1 mM) in a DMF solution of $TBAPF_6$ (0.1 M) using a glassy carbon electrode at 200 mV s^{-1} with 0 (black), 10 (red), 20 (green), 30 (blue), 40 (yellow), 50 (purple), 60 (orange) mM of acetic acid.

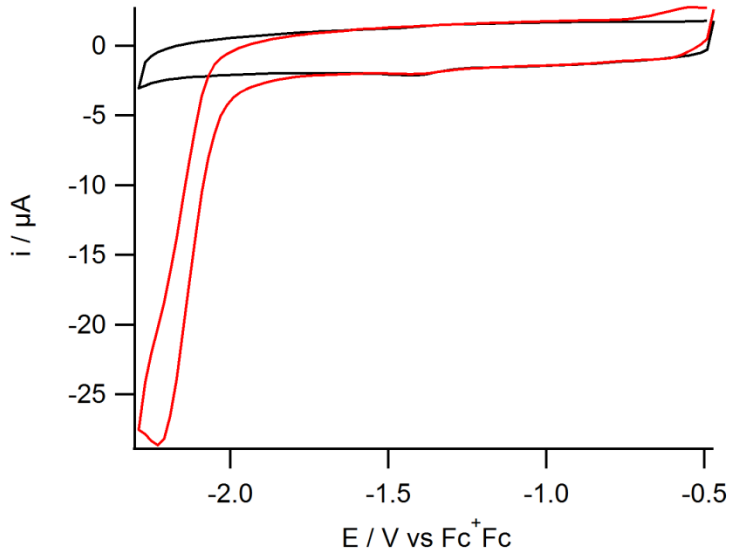

Figure AII.3: Cyclic voltammogram of [Ni(pbSmSe)] **(3)** (1 mM) in a DCM solution of $TBAPF_6$ (0.1 M) using a glassy carbon electrode at 200 mV s^{-1} (blank (black), [Ni(pbSmSe)] (red)).

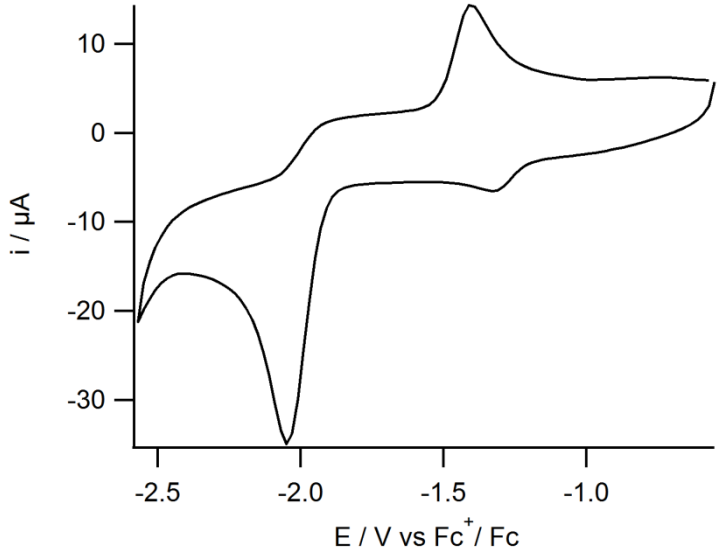

Figure AII.4: Cyclic voltammogram of $[FeCp(CO)_2I]$ (1 mM) in a DMF solution of $TBAPF_6$ (0.1 M) using a glassy carbon electrode at 200 mV s^{-1}.

Foot-of-the Wave Analysis

CV results were analyzed by using *FOWA* which helps to quantify the rates of HER. The observable rate constant (k_{obs}) can be obtained by plotting i/i_p^0 *vs* 1/1+exp[(F/RT)(E-E^0)] which gives a linear function at a certain scan rate. [2,3] For the complex **(5),** which has diffusion controlled reversible reaction, the current peaks (i and i_p^0) can be calculated according to equation (1) and (2): [2,3]

$$i_p^0 = 0.4463\text{FSC}_p^0\sqrt{\frac{F\nu D}{RT}} \qquad (1)$$

$$i = \frac{2\text{FS}C_p^0\sqrt{\frac{F\nu D}{RT}}}{1+\exp[\frac{F}{RT}(E-E^0)}} \qquad (2)$$

where i_p^0 =90.17 μA , F is the Faraday's constant, S the surface of electrode, C_p^0 the concentration of the complex in solution, D the diffusion coefficient, E^0 the half-wave potential of the redox couple triggering catalysis, R the gas constant and T the temperature. Combining equation (1) and (2) gives us equation (3) which shows us plotting i/i_p^0 *vs* 1/1+exp[(F/RT)(E-E^0)] gives access of the observed rate constant (k_{obs}).

$$\frac{i}{i_p^0} = \frac{\frac{2}{04463}\sqrt{\frac{RT(k_{obs})}{F\nu}}}{1+\exp[\frac{F}{RT}(E-E^0)]} \qquad (3)$$

i (μA)	i / i_p^0	1/1+exp[F/RT(E–E^0)]
20.25	0.225	022x10^{-4}
21.93	0.243	1.964x10^{-3}
24.38	0.270	4.269x10^{-3}
27.95	0.310	9.256x10^{-3}
32.74	0.363	0.01995
38.23	0.424	0.04247
43.53	0.483	0.0881
48.01	0.532	0.174

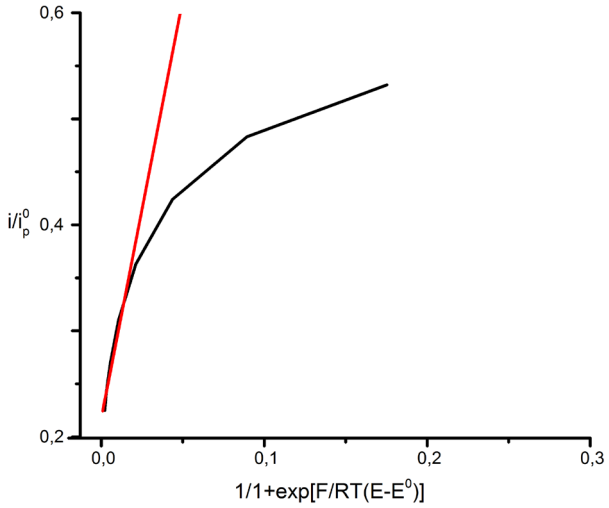

Figure AII.5: Plot of i/i_p^0 vs. 1/1+exp[F/RT(E−E^0)] using FOWA of the complex **(5)** for H_2 evolution at 200 mV s^{-1} and a concentration of HOAc of 60 mM. The experimental data (black) can be fitted linearly near the foot of the catalytic wave and the slope (red) gives the access to the observed rate constant k_{obs}= k × C_A^0 according to equation (4).[2] Equation (5)[2] gives us access to *k* which is 402 $M^{-1}s^{-1}$ and k_{obs} is 24 s^{-1}.

$$slope = \frac{2}{0.4463}\sqrt{(k_{obs})\frac{RT}{Fv}} \qquad (4)$$

$$k = \frac{slope^2 (0.4463)^2 Fv}{4RTC_A^0} \qquad (5)$$

H_2 evolution calculations are based on a calibration line obtained by the external reference method by injection of known amounts of H_2 into the system (Figure.AI2). During the CPC experiment hydrogen is only produced from the local concentration of catalyst at the electrode surface. For this measurement, a glassy carbon electrode with 3 mm diameter was used. After 50 min the area of the H_2 peak is 4054 for the complex **(5)** and according to the equation from calibration line (Fig.AI.3):

y = (0.01649x4054)−2.99413 = 64 µl H_2

$(64x10^{-6})÷(24.465) = 2.62x10^{-6}$ mol H_2

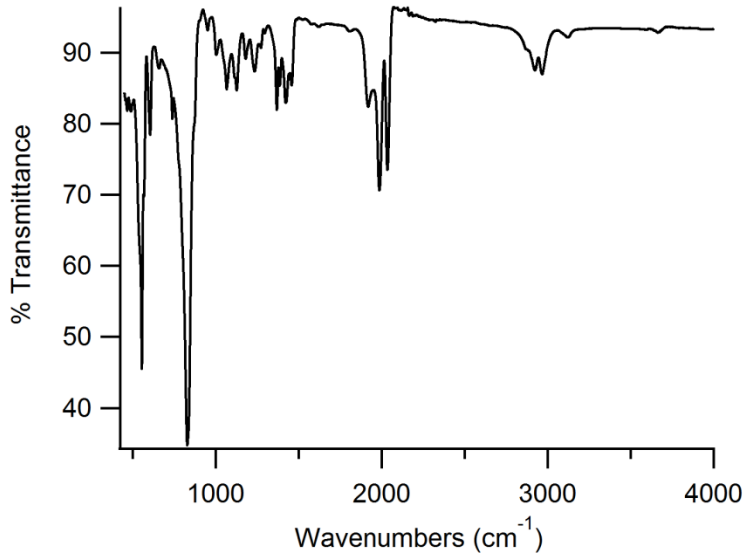

Figure AII.6: FTIR spectrum of the complex **(5)**.

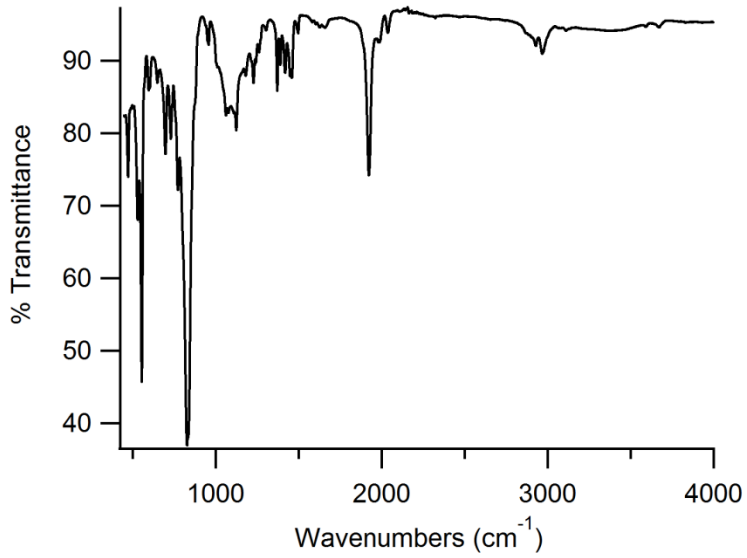

Figure AII.7: FTIR spectrum of the complex **(6)**.

References

1. G. M. Sheldrick, *Acta Cryst.,* 2015, **C71**, 3.
2. C. Costentin, S. Drouet, M. Robert and J. M. Savéant, *J. Am. Chem. Soc.* 2012, **134**, 11235.
3. N. Elgrishi, B. M. Chambers and M. Fontecave, *Chem. Sci.* 2015**, 6**, 2522.

Appendix III

Supplementary Information on Chapter 3

Table AIII.1: Crystal and structure refinement data for complexes **(1)** and **(2)**

Experiments were carried out at 110 K using a SuperNova, Dual, Cu at zero, Atlas. H-atom parameters were constrained.

	(1)	**(2)**
Crystal data		
Chemical formula	$2(C_{39}H_{44}NiPRuS_4)\cdot 2(F_6P)\cdot C_5H_{12}$	$2(C_{39}H_{44}NiPRuS_2Se_2)\cdot 2(F_6P)\cdot C_5H_{12}$
M_r	2025.54	2213.14
Crystal system, space group	Triclinic, *P*−1	Triclinic, *P*−1
a, *b*, *c* (Å)	10.4124 (3), 13.6997 (3), 16.9554 (5)	10.4311 (2), 13.7933 (3), 17.0273 (3)
α, β, γ (°)	71.664 (2), 86.558 (2), 69.587 (2)	71.685 (2), 86.5782 (17), 69.258 (2)
V (Å^3)	2148.30 (11)	2171.35 (8)
Z	1	1
Radiation type	Cu *K*α	Cu *K*α
μ (mm^{-1})	6.39	7.34
Crystal size (mm)	0.23 × 0.17 × 0.02	0.17 × 0.13 × 0.03

	(1)	(2)
Data collection		
Absorption correction	Analytical *CrysAlis PRO*, Agilent Technologies, Version 1.171.36.32 (release 02-08-2013 CrysAlis171 .NET) (compiled Aug 2 2013,16:46:58) Analytical numeric absorption correction using a multifaceted crystal model based on expressions derived by R.C. Clark & J.S. Reid. (Clark, R. C. & Reid, J. S. (1995). Acta Cryst. A51, 887-897)[1]	Analytical *CrysAlis PRO*, Agilent Technologies, Version 1.171.36.32 (release 02-08-2013 CrysAlis171 .NET) (compiled Aug 2 2013,16:46:58) Analytical numeric absorption correction using a multifaceted crystal model based on expressions derived by R.C. Clark & J.S. Reid. (Clark, R. C. & Reid, J. S. (1995). Acta Cryst. A51, 887-897)[1]
T_{min}, T_{max}	0.436, 0.866	0.408, 0.833
No. of measured, independent and observed [$I > 2\sigma(I)$] reflections	27501, 8405, 7525	27022, 8480, 7577
R_{int}	0.039	0.033
$(\sin \theta/\lambda)_{max}$ (Å^{-1})	0.617	0.616
$R[F^2 > 2\sigma(F^2)]$, $wR(F^2)$, S	0.028, 0.073, 1.03	0.029, 0.074, 1.06
No. of reflections	8405	8480
No. of parameters	731	719
No. of restraints	875	851
Δ_{max}, $\Delta\rangle_{min}$ (e Å^{-3})	0.57, -0.57	0.64, -0.61

Computer programs: *CrysAlis PRO*, Agilent Technologies, Version 1.171.36.32 (release 02-08-2013 CrysAlis171 .NET) (compiled Aug 2 2013, 16:46:58), *SHELXS2014*/7 (Sheldrick, 2015), *SHELXL2014*/7 (Sheldrick, 2015), *SHELXTL* v6.10 (Sheldrick, 2008).[2]

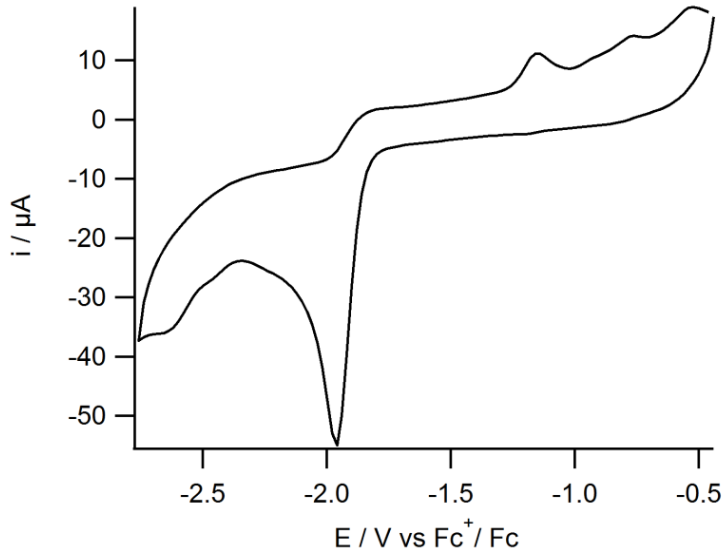

Figure AIII.1: Cyclic voltammogram of [Ni(xbSmS)] (1 mM) in an MeCN solution containing $TBAPF_6$ (0.1 M) as the supporting electrolyte and using a glassy carbon electrode at 200 mV s^{-1}.

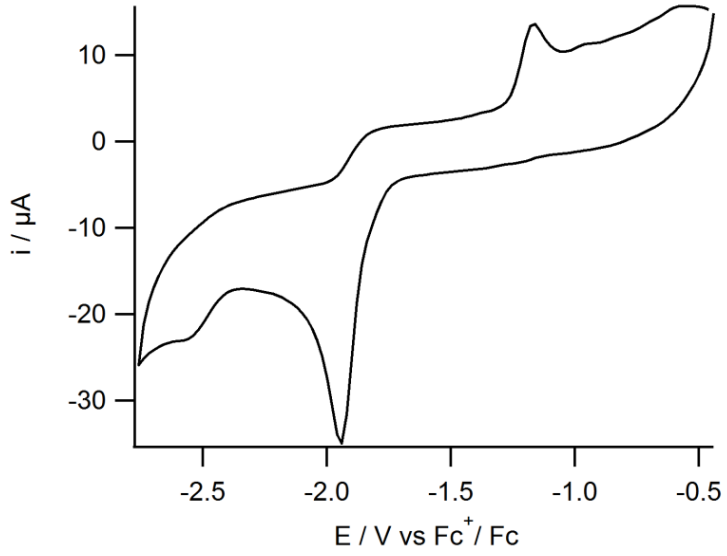

Figure AIII.2: Cyclic voltammogram of [Ni(xbSmSe)] (1 mM) in an MeCN solution containing $TBAPF_6$ (0.1 M) as the supporting electrolyte and using a glassy carbon electrode at 200 mV s^{-1}.

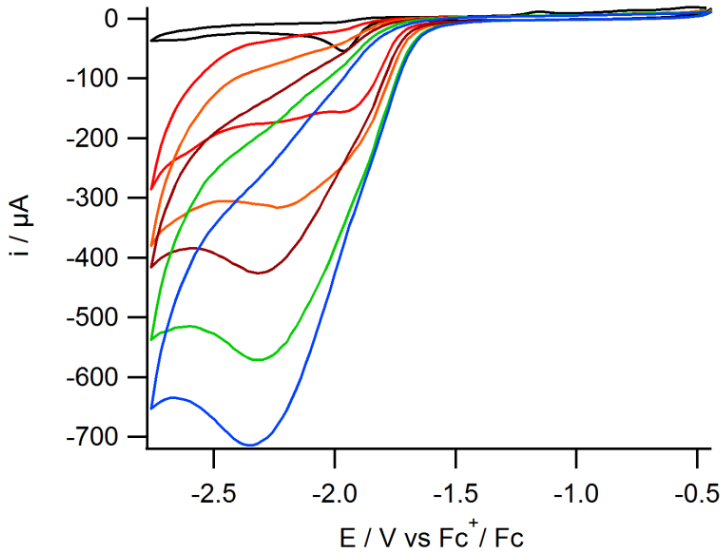

Figure AIII.3: Cyclic voltammogram of [Ni(xbSmS)] (1 mM) in an MeCN solution containing $TBAPF_6$ (0.1 M) as the supporting electrolyte and using a glassy carbon electrode at 200 mV s^{-1} in the presence of 0 (black), 10 (red), 20 (orange), 30 (brown), 40 (green), 50 (blue) mM of acetic acid.

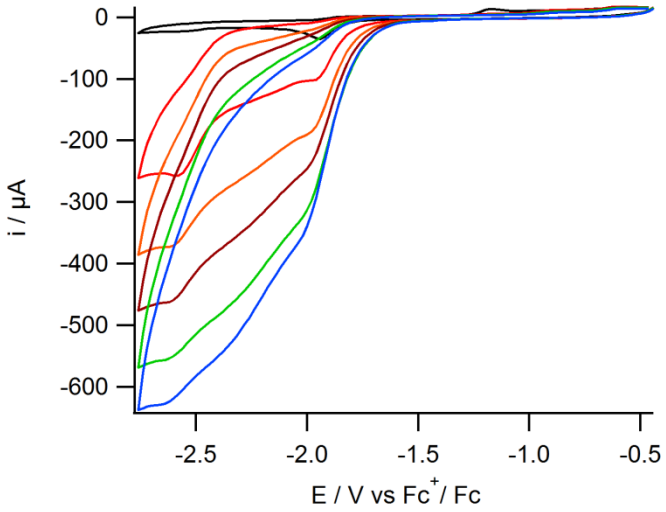

Figure AIII.4: Cyclic voltammogram of [Ni(xbSmSe)] (1 mM) in an MeCN solution containing $TBAPF_6$ (0.1 M) as the supporting electrolyte and using a glassy carbon electrode at 200 mV s^{-1} in the presence of 0 (black), 10 (red), 20 (orange), 30 (brown), 40 (green), 50 (blue) mM of acetic acid.

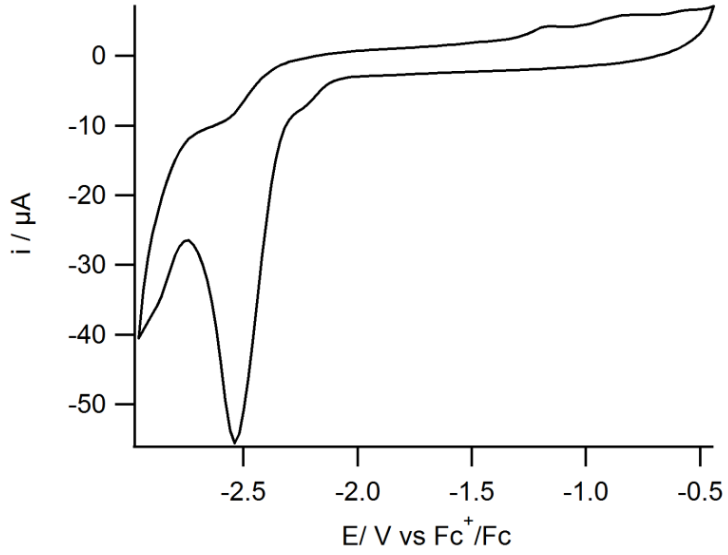

Figure AIII.5: Cyclic voltammogram of **[**$RuCp(PPh_3)(MeCN)_2]PF_6$ (1 mM) in an MeCN solution containing $TBAPF_6$ (0.1 M) as the supporting electrolyte and using a glassy carbon electrode at 200 mV s^{-1}.

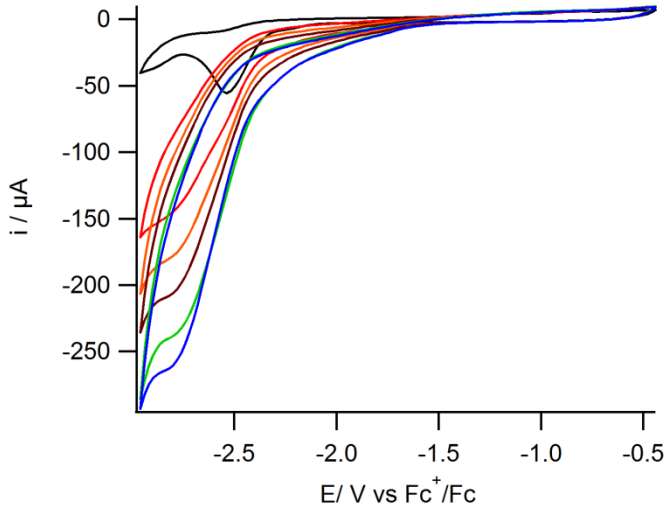

Figure AIII.6: Cyclic voltammogram of **[**$RuCp(PPh_3)(MeCN)_2]PF_6$ (1 mM) in an MeCN solution containing $TBAPF_6$ (0.1 M) as the supporting electrolyte and using a glassy carbon electrode at 200 mV s^{-1} in the presence of 0 (black), 10 (red), 20 (orange), 30 (brown), 40 (green), 50 (blue) mM of acetic acid.

References

1. R.C. Clark and J.S. Reid, *Acta Cryst.*, 1995, **A51**, 887.
2. G. M. Sheldrick, *Acta Cryst.,* 2015, **C71**, 3.

Appendix IV

Supplementary Information on Chapter 4

Table AIV.1: Crystal and structure refinement data for complexes **(1)**, **(2)**, **(4)** and **(6)**

Data were collected at 110 K for **(1)**, **(4)** and **(6)**, at 150 K for **(2)**

	(1)	**(2)**	**(4)**	**(6)**
Chemical formula	$C_{20}H_{40}Ni_2S_8$ CH_2Cl_2	$C_{12}H_{24}Ni_2S_6$	$C_{14}H_{28}Ni_2S_4Se_2$	$C_{12}H_{24}Ni_2S_4Se_2$
M_r	739.35	478.09	599.94	571.89
Crystal system, space group	Orthorhombic, *Pna2₁*	Orthorhombic, *Pbca*	Orthorhombic, *Pna*2₁	Orthorhombic, *Pbca*
a, *b*, *c* (Å)	10.5534(3), 23.6789(8), 12.4717(3)	12.9460(1), 22.3503(2), 12.9344(1)	12.08190 (17), 14.03764 (18), 12.21318 (17)	12.8544 (2), 13.3702 (3), 22.4216 (5)
V (Å^3)	3116.58(16)	3742.53(5)	2071.37 (5)	3853.51 (14)
Z	4	8	4	8
μ (mm^{-1})	1.93	2.67	9.98	10.69
Data collection				
R_{int}	0.042	0.046	0.018	0.038
$(\sin\theta/\lambda)_{max}$ (Å^{-1})	0.61	0.65	0.616	0.616
Refinement				
No. of reflections	5617	3733	3211	3771
No. of parameters	346	185	204	185
$\Delta\rho_{max}$,$\Delta\rho_{min}$ (e Å^{-3})	0.82, -0.38	0.49, -0.38	0.80, −0.54	0.44, −0.34

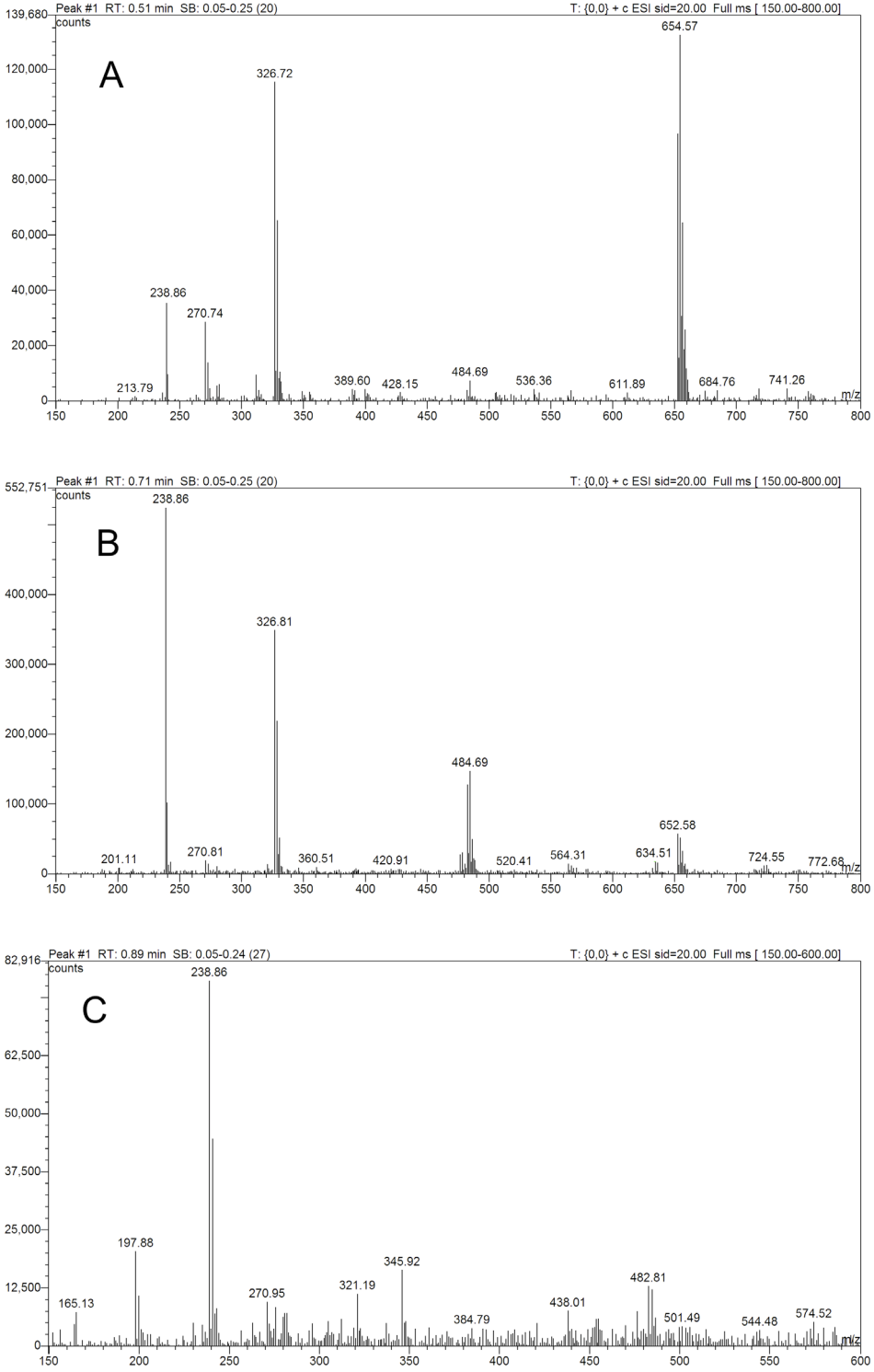

Figure AIV.1. Formation of $[Ni_2(emSmS)_2]$ **(2)** from $[Ni_2(ebSmS)_2]$ **(1)**, as monitored with ESI-MS spectrometry upon irradiation on the toluene solution of $[Ni_2(ebSmS)_2]$ **(1)** at room temperature; (A) 0 hrs, (B) 6 hrs, (C) 12 hrs; *m/z* = 326.72 = $[Ni(ebSmS)+H]^+$, 652.57 = $[\{Ni(ebSmS)\}_2+H]^+$ and 238.86 = $[Ni(emSmS)+H]^+$.

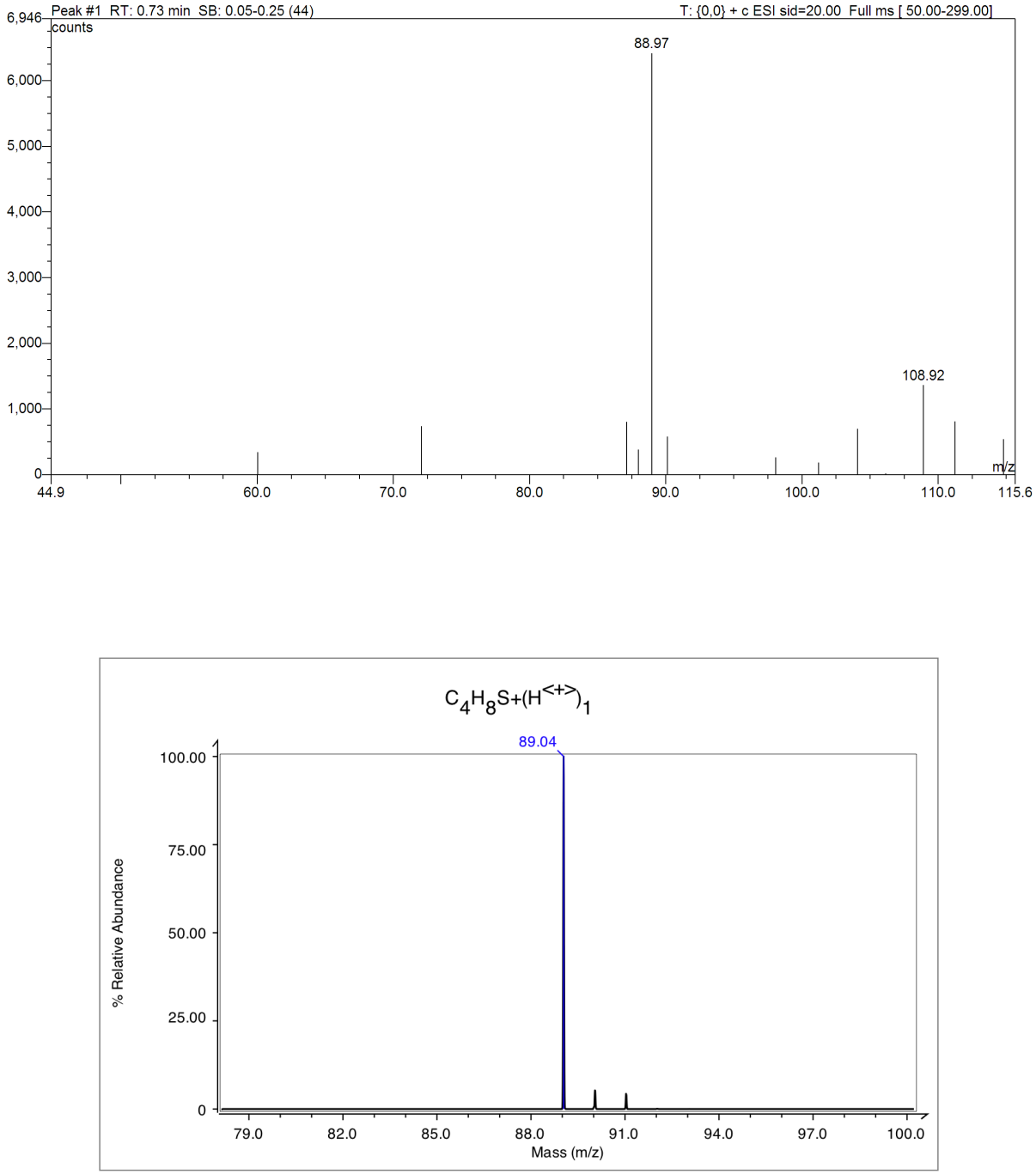

Figure AIV.2. ESI-MS of (poly)isobutylene sulfide in dichloromethane, extracted from the reaction of **(1)** upon irradiation on the toluene solution (top) and the signal simulated for $[C_4H_8S+H]^+$ (bottom).

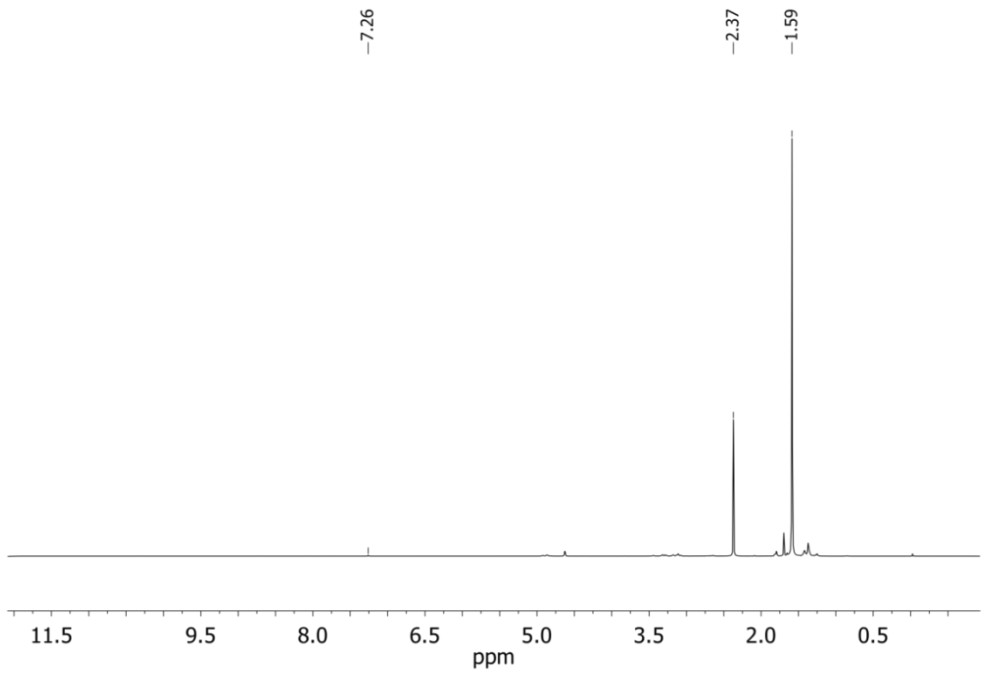

Figure AIV.3. ^{1}H NMR spectrum of isobutylene sulfide isolated after the photolysis of complex (1); recorded using CD_2Cl_2 solution at 298 K.

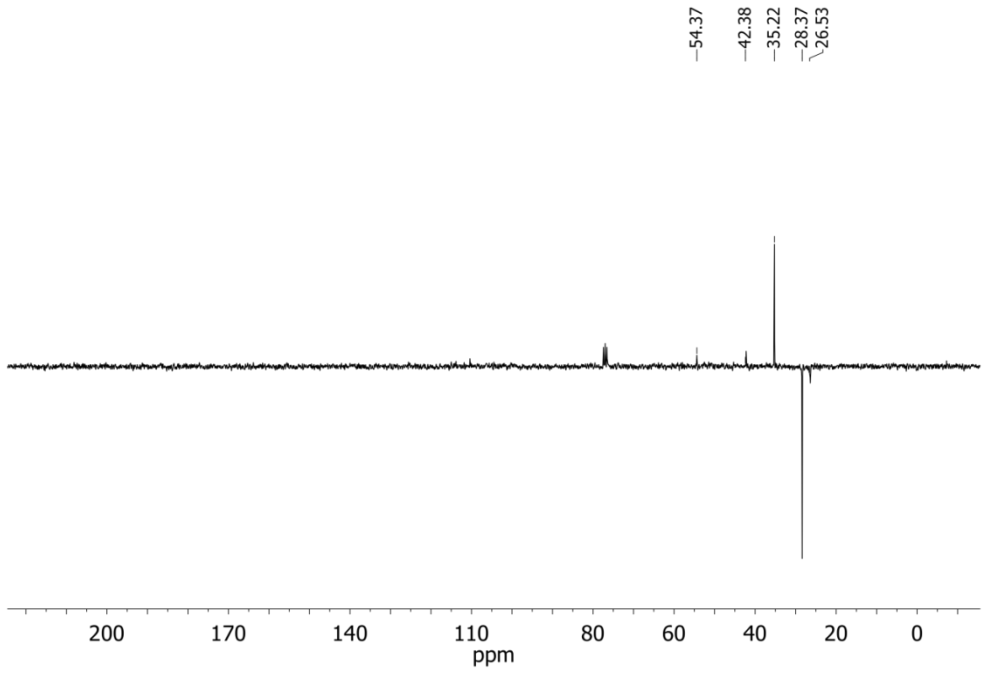

Figure AIV.4. ^{13}C NMR (APT) spectrum of isobutylene sulfide isolated after the photolysis of complex (1); recorded using CD_2Cl_2 solution at 298 K.

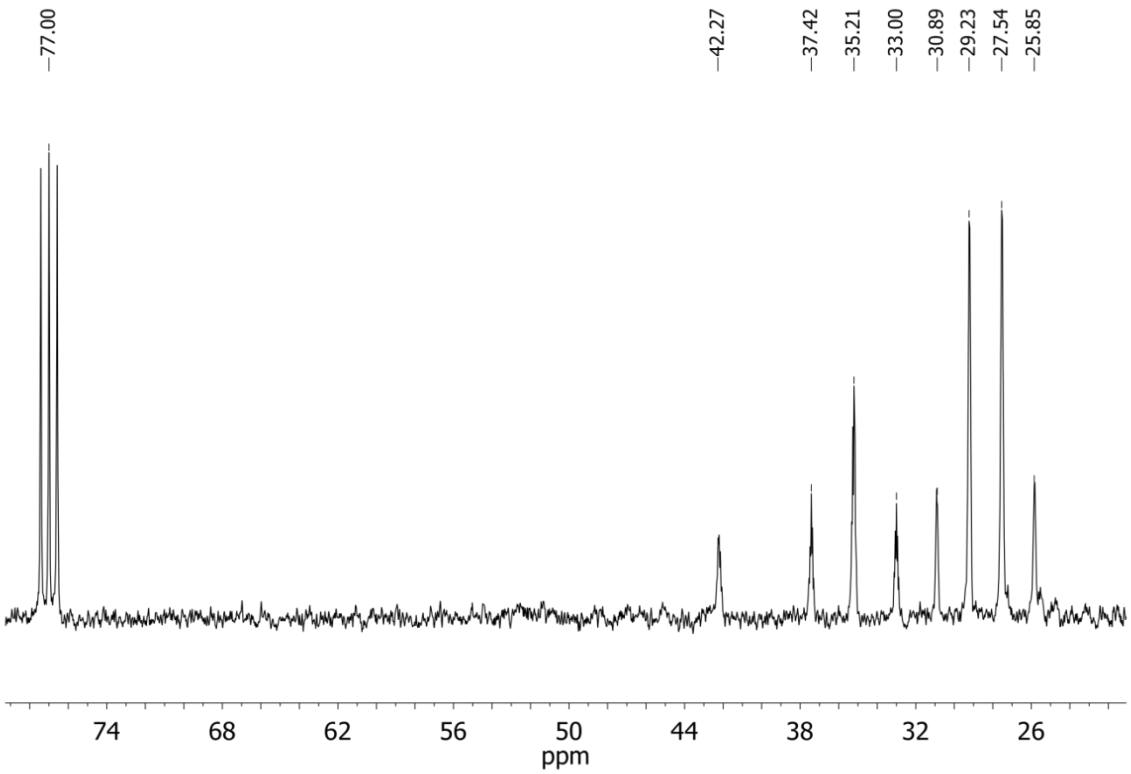

Figure AIV.5. ^{13}C NMR (gated decoupled) spectrum of isobutylene sulfide isolated after photolysis of complex **(1)**, recorded using CD_2Cl_2 solution at 298 K.

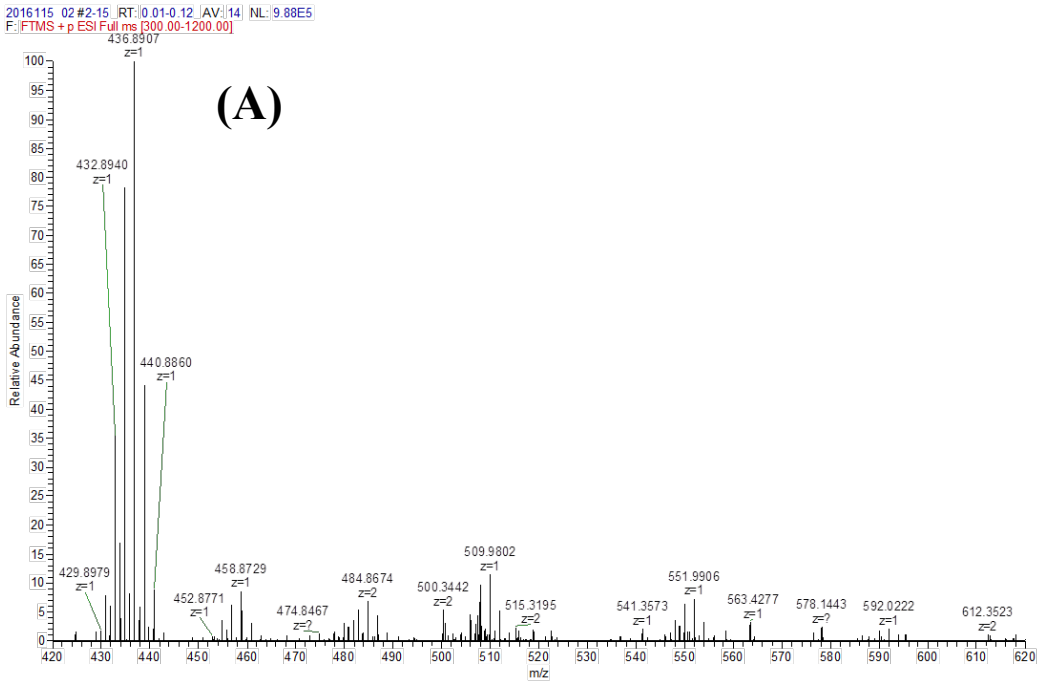

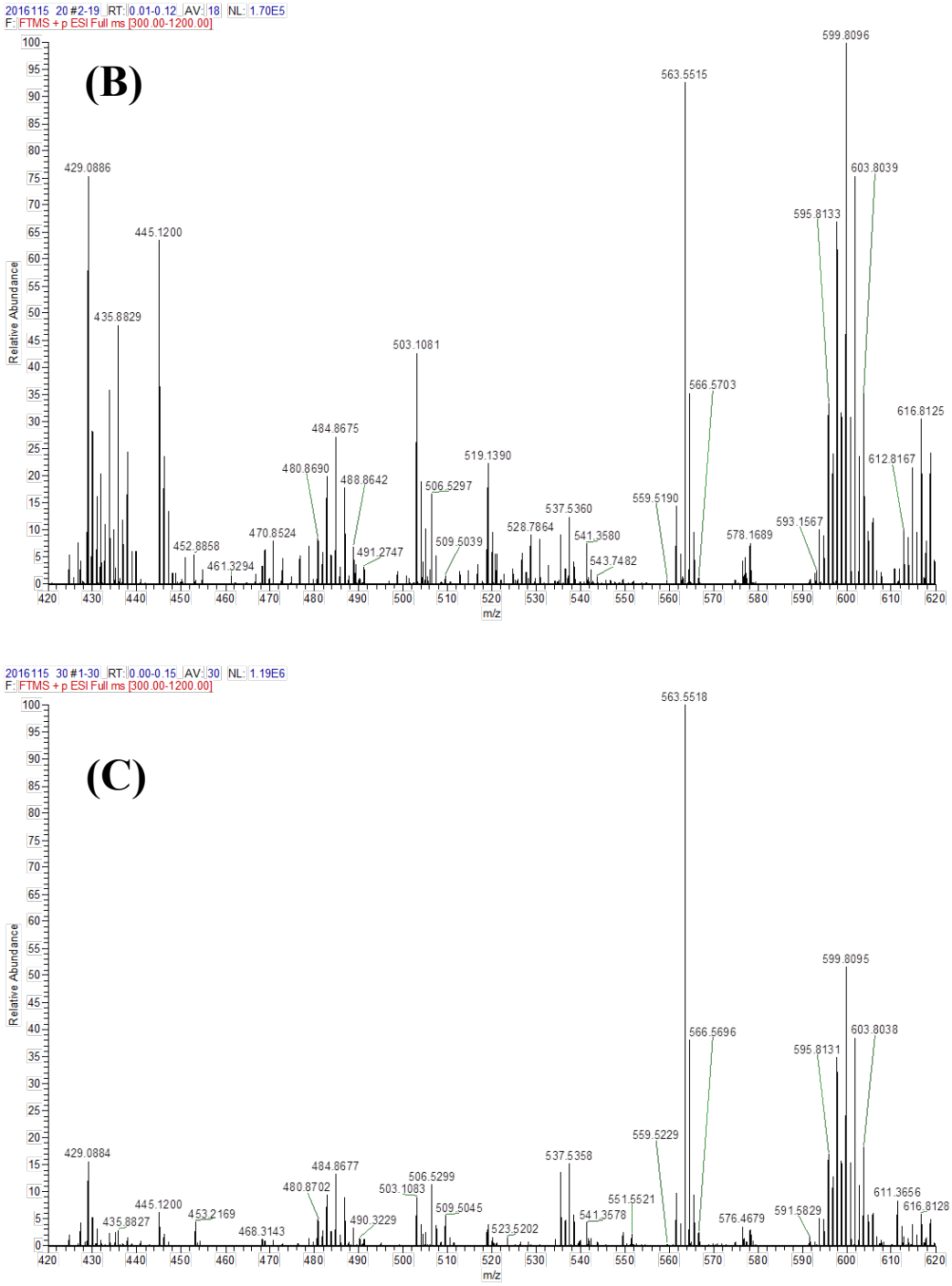

Figure AIV.6. Formation of $[Ni_2(pmSmSe)_2]$ **(4)** from [Ni(pbSmSe)] **(3)**, as monitored with HRMS spectrometry upon irradiation of the dichloromethane solution of [Ni(pbSmSe)] **(3)** at room temperature; (A) 0 hrs, (B) 1 h (C) 2 h *m/z* = 436.8846 = $[Ni(pbSmSe)+H]^+$, *m/z* =599.8111 = $[Ni_2(pmSmSe)_2]$, signals present in the blank from solvent: 509.33 and 563.55.

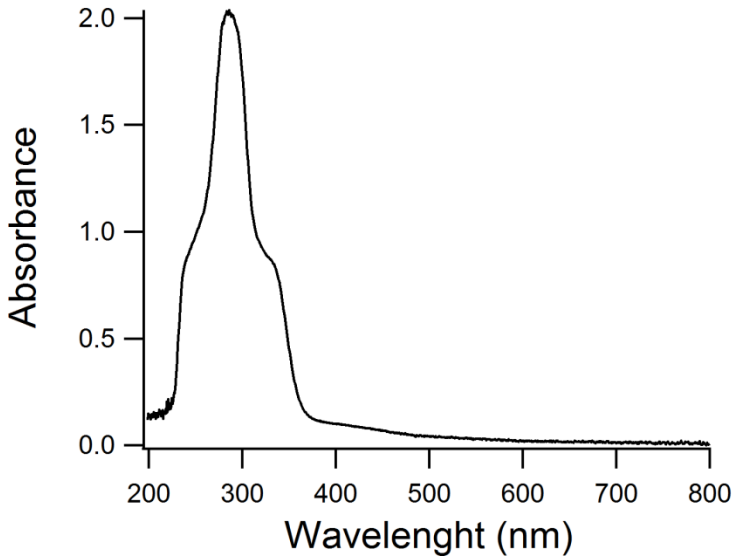

Figure AIV.7. UV-VIS spectrum of complex **(3)** (1 mM) in dichloromethane. The spectrum was recorded with a transmission dipprobe set at a path length of 2 mm.

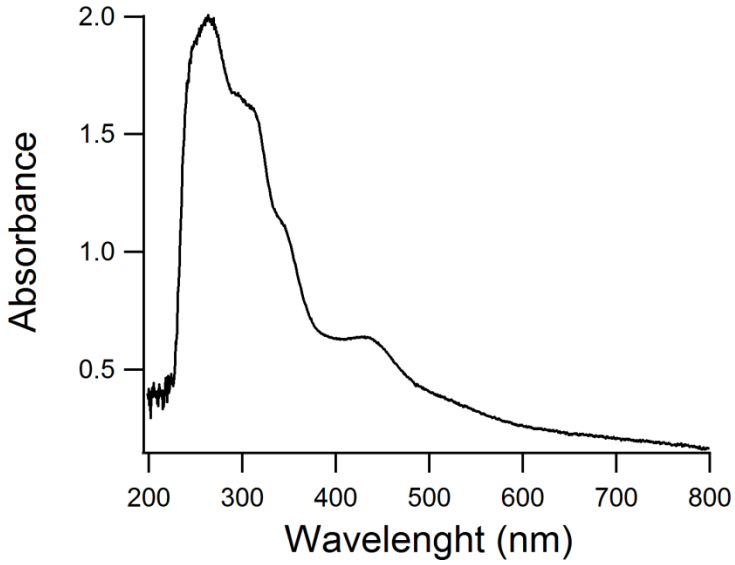

Figure AIV.8. UV-VIS spectrum of complex **(4)** (1 mM) in dichloromethane. The spectrum was recorded with a transmission dipprobe set at a path length of 2 mm.

Appendix V

Supplementary Information on Chapter 5

Table AV.1: Crystal and structure refinement data for complexes **(1)** and **(2)**

Data were collected at 110 K using a SuperNova, Dual, Cu and Mo at zero, Atlas. H-atom parameters were constrained.

	(1)	**(2)**
Crystal data		
Chemical formula	$C_{56}H_{64}N_4Ni_2RuS_8 \cdot 2(F_6P) \cdot 1.437(C_3H_6O)$	$C_{56}H_{64}N_4Ni_2RuS_4Se_4 \cdot 2(F_6P) \cdot 1.387(C_3H_6O)$
M_r	1641.43	1826.21
Crystal system, space group	Triclinic, *P*-1	Triclinic, *P*-1
a, *b*, *c* (Å)	10.0605(3), 17.5378(5), 21.7349(6)	10.1408(2), 18.4675(4), 20.4960(5)
α, β, γ (°)	109.731(3), 96.492(2), 106.004(3)	109.249(2), 98.2255(19), 105.4158(19)
V (Å^3)	3378.57(19)	3379.33(14)
Z	2	2
Radiation type	Cu *K*α	Mo *K*α
μ (mm^{-1})	5.87	3.18
Crystal size (mm)	0.35 × 0.05 × 0.03	0.38 × 0.08 × 0.06

	(1)	(2)
Data collection		
Absorption correction	Analytical *CrysAlis PRO*, Agilent Technologies, Version 1.171.36.32 (release 02-08-2013 CrysAlis171 .NET) (compiled Aug 2 2013,16:46:58) Analytical numeric absorption correction using a multifaceted crystal model based on expressions derived by R.C. Clark & J.S. Reid. (Clark, R. C. & Reid, J. S. (1995). Acta Cryst. A51, 887-897)[1]	Gaussian *CrysAlis PRO*, Agilent Technologies, Version 1.171.36.32 (release 02-08-2013 CrysAlis171 .NET) (compiled Aug 2 2013,16:46:58) Numerical absorption correction based on gaussian integration over a multifaceted crystal model.
T_{min}, T_{max}	0.310, 0.834	0.461, 1.000
No. of measured, independent and observed [$I > 2\sigma(I)$] reflections	32405, 13234, 10915	51473, 15498, 12221
R_{int}	0.033	0.039
$(\sin \theta/\lambda)_{max}$ (Å^{-1})	0.617	0.649
$R[F^2 > 2\sigma(F^2)]$, $wR(F^2)$, S	0.036, 0.093, 1.02	0.035, 0.080, 1.02
No. of reflections	13234	15498
No. of parameters	1333	1044
No. of restraints	1848	1021
$\Delta\rho_{max}$, $\Delta\rho_{min}$ (e Å^{-3})	1.04, -1.20	1.06, -0.74

Computer programs: *CrysAlis PRO*, Agilent Technologies, Version 1.171.36.32 (release 02-08-2013 CrysAlis171 .NET) (compiled Aug 2 2013, 16:46:58), *SHELXS2014*/7 (Sheldrick, 2015), *SHELXS2014*/7 (Sheldrick, 2014), *SHELXL2014*/7 (Sheldrick, 2015), *SHELXL2014*/7 (Sheldrick, 2014), *SHELXTL* v6.10 (Sheldrick, 2008).[2]

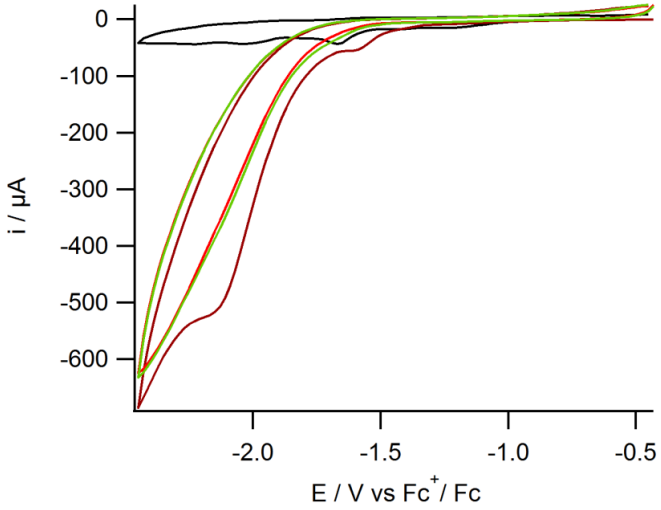

Figure AV.1: Cyclic voltammograms of $[\{Ni(xbSmS)\}_2Ru(phen)_2](PF_6)_2$ (1 mM) in acetonitrile solution containing $TBAPF_6$ (0.1 M) as the supporting electrolyte and using a glassy carbon electrode at 200 mV s^{-1} without acid (black), in the presence of 50 mM acid with three different scans: brown (1st scan), green (2nd scan) and red (3rd scan).

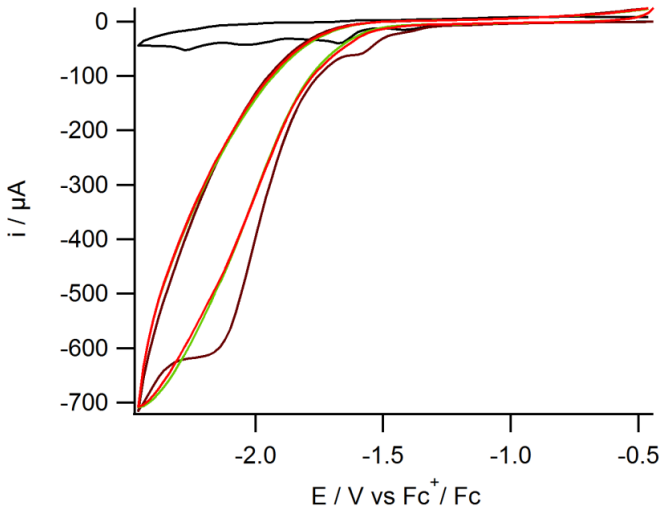

Figure AV.2: Cyclic voltammograms of $[\{Ni(xbSmSe)\}_2Ru(phen)_2](PF_6)_2$ (1 mM) in acetonitrile solution containing $TBAPF_6$ (0.1 M) as the supporting electrolyte and using a glassy carbon working electrode at 200 mV s^{-1} without acid (black), in the presence of 50 mM acid with three different scans: brown (1st scan), green (2nd scan) and red (3rd scan).

References

1. R.C. Clark and J.S. Reid, *Acta Cryst.*, 1995, **A51**, 887.
2. G. M. Sheldrick, *Acta Cryst.,* 2015, **C71**, 3.